C–I NC halogen bonding in two polymorphs of the mixed-valence 2:1 charge-transfer salt (EDTTTF-I2)2(TCNQF4), with segregated versus alternated stacks

Julien Lieffrig, Olivier Jeannin, Antoine Vacher, Dominique Lorcy, Pascale Auban-Senzier, Marc Fourmigué

Acta Crystallographica Section B
Structural Science, Crystal Engineering and Materials
ISSN 2052-5206

C—I···NC halogen bonding in two polymorphs of the mixed-valence 2:1 charge-transfer salt (EDT-TTF-I_2)$_2$($TCNQF_4$), with segregated *versus* alternated stacks

Julien Lieffrig,[a] Olivier Jeannin,[a] Antoine Vacher,[a] Dominique Lorcy,[a] Pascale Auban-Senzier[b] and Marc Fourmigué[a]*

[a]Institut des Sciences Chimiques de Rennes, Université Rennes 1, UMR CNRS 6226, Campus de Beaulieu, 35042 Rennes, France, and [b]Laboratoire de Physique des Solides, Université Paris-Sud, UMR CNRS 8502, Bât. 510, 91405 Orsay, France

Correspondence e-mail: marc.fourmigue@univ-rennes1.fr

Received 16 September 2013
Accepted 30 November 2013

Oxidation of diiodoethylenedithiotetrathiafulvalene (EDT-TTF-I_2), $C_8H_4I_2S_6$, with the strong oxidizer tetrafluorotetracyanoquinodimethane ($TCNQF_4$), $C_{12}F_4N_4$, affords, depending on the crystallization solvent, two polymorphs of the 2:1 charge-transfer salt (EDT-TTF-I_2)$_2$($TCNQF_4$), represented as D_2A. In both salts, the $TCNQF_4$ is reduced to the radical anion state, and is associated through short C—I···NC halogen bonds to two EDT-TTF-I_2 molecules. The two polymorphs differ in the solid-state association of these trimeric *D*–*A*–*D* motifs. In polymorph (I) the trimeric motif is located on an inversion centre, and hence both EDT-TTF-I_2 molecules have +0.5 charge. Together with segregation of the TTF and TCNQ derivatives into stacks, this leads to a charge-transfer salt with high conductivity. In polymorph (II) two crystallographically independent EDT-TTF-I_2 molecules bear different charges, close to 0 and +1, as deduced from an established correlation between intramolecular bond lengths and charge. Overlap interactions between the halogen-bonded D^0–$A^{-\bullet}$–$D^{+\bullet}$ motifs give rise, in a perpendicular direction, to diamagnetic A_2^{2-} and D^0–D_2^{2+}–D^0 entities, where the radical species are paired into the bonding combination of respectively the acceptor LUMOs and donor HOMOs. The strikingly different solid-state organization of the halogen-bonded *D*–*A*–*D* motifs provides an illustrative example of two modes of face-to-face interaction between π-type radicals, into either delocalized, uniform chains with partial charge transfer and conducting behaviour, or localized association of radicals into face-to-face A_2^{2-} and D_2^{2+} dyads.

1. Introduction

Halogen bonding is an effective and reliable tool in solid-state supramolecular chemistry, as described by Metrangolo *et al.* (2008), and Metrangolo & Resnati (2001, 2012). It has been extensively investigated in supramolecular chemistry (Meyer & Dubois, 2013; Gilday *et al.*, 2013), but also for the elaboration of liquid crystals (Nguyen *et al.*, 2004; Metrangolo *et al.*, 2006; Präsang *et al.*, 2008) and gels (Meazza *et al.*, 2013), anion sensors (Metrangolo *et al.*, 2009; Cavallo *et al.*, 2010), catalytic systems (Bruckmann *et al.*, 2008; Walter *et al.*, 2011; Kniep *et al.*, 2013) nonlinear optical (Cariati *et al.*, 2007) or magnetic/conductive materials (Fourmigué & Batail, 2004; Fourmigué, 2008). Such halogen-bonded conductive materials are most often based on an iodinated tetrathiafulvalene molecule (Gompper *et al.*, 1995; Wang *et al.*, 1994) such as EDT-TTF-I. The electrocrystallization of EDT-TTF-I in the presence of various counter ions affords mixed-valence salts, formulated as (EDT-TTF-I)$_2X$ [X = Br^-, $Ag(CN)_2^-$ *etc.*], where X acts both as an anion to compensate the partial positive charge of the donor molecules, and as a halogen-bond

acceptor towards the I atom of EDT-TTF-I (Imakubo *et al.*, 1995; Ueda *et al.*, 2003; Ranganathan *et al.*, 2006). The overlap interactions between TTF molecules, perpendicular to this trimeric motif, lead to the formation of conduction bands. Partial filling, due to the stoichiometry, and large band dispersion are the necessary conditions for metallic behaviour (Fourmigué, 2012).

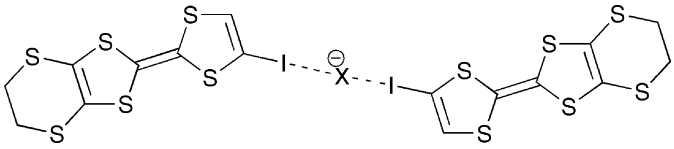

Besides such cation radical salts with electrochemically innocent anions, it is also possible to consider the chemical formation of charge-transfer salts, where the anion itself is electroactive, from the oxidation of the TTF derivative with an organic oxidant. Within this frame, a series of charge-transfer salts of EDT-TTF-I was recently reported, with a variety of tetracyanoquinodimethane (TCNQ) derivatives of different oxidative ability, *i.e.* $TCNQF_4 > TCNQF_2 > TCNQF > TCNQ$ (Lieffrig, Jeannin, Guizouarn *et al.*, 2012). While a neutral charge-transfer complex was isolated with the weaker acceptor TCNQ, an intermediate mixed-valence salt was found with $TCNQF_2$ and a full charge-transfer salt with $TCNQF_4$. Surprisingly, however, while $C_{TTF}-I\cdots N{\equiv}C$ halogen bonds were observed in the mixed-valence salts, where the donor charge, $\rho_{EDT\text{-}TTF\text{-}I}$, amounts to +0.5, and also in the neutral TCNQ complex [$\rho_{EDT\text{-}TTF\text{-}I} = 0$], they are surprisingly absent from the full charge-transfer salt with $TCNQF_4$. It was shown that TTF oxidation also activates the TTF sp^2 H atom located directly adjacent (α) to the I atom towards the preferential formation of $C_{TTF}-H_{\alpha}\cdots N{\equiv}C$ hydrogen bonds. These series provided an opportunity to evaluate the relative strength of competing $C-H\cdots N$ hydrogen and $C-I\cdots N$ halogen bonds and demonstrated that halogen bonding is not as sensitive as $C-H\cdots N$ hydrogen bonding to the charge of the TTF core (Lieffrig, Jeannin, Guizouarn *et al.*, 2012).

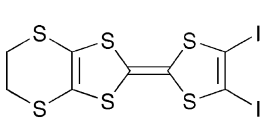

EDT-TTF-I_2

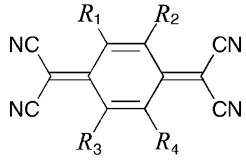

TCNQ R_1–R_4 = H
TCNQF R_1 = F, R_2–R_4 = H
$TCNQF_2$ R_1,R_4 = F, R_2,R_3 = H
$TCNQF_4$ R_1–R_4 = F

In the present work, we wanted to suppress this halogen bond/hydrogen bond competition and accordingly concentrated on the analogous diiodotetrathiafulvalene derivative, namely EDT-TTF-I_2. Because of the presence of two electron-withdrawing I atoms, EDT-TTF-I_2 oxidizes at a rather high potential (0.57 V *versus* SCE; SCE = saturated calomel electrode), and only a few charge-transfer salts have been described to date, for example with the strong electron acceptor 2,3-dichloro-5,6-dicyano-1,4-benzoquinone (DDQ; Lieffrig, Jeannin, Shin *et al.*, 2012), although many cation radical salts were obtained by electrochemical oxidation (electrocrystallization; Domercq *et al.*, 2001; Devic *et al.*, 2002, 2003; Alberola *et al.*, 2008; Fourmigué & Auban-Senzier, 2008; Shin *et al.*, 2011). In the DDQ charge-transfer salt formulated as $(EDT\text{-}TTF\text{-}I_2)_2(DDQ)$, halogen-bonding interactions were observed toward both the O atom of the carbonyl and the N atom of the nitrile groups of reduced DDQ. In addition, a segregation of the partially oxidized EDT-TTF-I_2 molecules into layers allowed for the formation of conducting slabs, with a room-temperature conductivity of 0.043 S cm^{-1}. Looking for other possible oxidants comparable to DDQ, we turned our attention to fluorinated TCNQ derivatives. Indeed, because of the electron-withdrawing nature of F, the mono-, di- and tetrafluoro analogues of TCNQ, namely TCNQF, $TCNQF_2$ and $TCNQF_4$, exhibit a reduction potential higher than that of TCNQ itself (+0.14 V *versus* SCE) and increasing with the number of F atoms, that is +0.26 V in TCNQF, +0.30 V for $TCNQF_2$, +0.53 V for $TCNQF_4$ (all *versus* SCE). Reaction of EDT-TTF-I_2 with TCNQ, TCNQF and $TCNQF_2$ afforded a series of isostructural compounds, where the degree of charge transfer was found to vary with the acceptor ability of $TCNQF_n$ (Lieffrig *et al.*, 2013). On the other hand, the stronger oxidant $TCNQF_4$ afforded two charge-transfer salts, both formulated as $(EDT\text{-}TTF\text{-}I_2)_2(TCNQF_4)$, with strikingly different solid-state organizations of the halogen-bonded $EDT\text{-}TTF\text{-}I_2^{+\bullet}$ and $TCNQF_4^{-\bullet}$ radical species. These two polymorphs described herein illustrate the two main modes of solid-state organization of π-type radical species (Fourmigué, 2012), either in extended delocalized chains with the possibility for conductivity or into dimeric or tetrameric units with localized bonding interactions.

2. Experimental

2.1. Materials and methods

$TCNQF_4$ was prepared according to a literature procedure (Wheland & Martin, 1975). The neutral EDT-TTF-I_2 molecule was prepared as previously described (Domercq *et al.*, 2001), and recrystallized by slow evaporation from a CS_2 solution, to provide crystals suitable for X-ray diffraction experiments. Since this reported synthetic procedure provides EDT-TTF-I_2 only in low yield, we also explored an alternative synthetic path that had been used for the analogous dibromo derivative (Batsanov *et al.*, 2001; Alberola *et al.*, 2006). Full details of this synthesis are described in the supporting information,[1] together with the crystal structure of one of the synthesis intermediates, $[NC(CH_2)_2S]_2TTFI_2$.

2.2. Synthesis of the charge-transfer salts

2.2.1. Polymorph (I). In a small glass tube of internal diameter 5 mm, a solution of EDT-TTF-I_2 (6.1 mg, 13×10^{-6} mol) in dichloromethane was layered with a solution of

[1] Supporting information for this paper is available from the IUCr electronic archives (Reference: BI5028).

Table 1
Experimental details.

Experiments were carried out with Mo $K\alpha$ radiation. Absorption was corrected for by multi-scan methods, *SADABS* (Bruker, 2003). H-atom parameters were constrained.

	$[NC(CH_2)_2S]_2$-TTF-I_2	EDT-TTF-I_2	(I)	(II)
Crystal data				
Chemical formula	$C_{12}H_8I_2N_2S_6$	$C_8H_4I_2S_6$	$C_{12}F_4N_4{\cdot}2C_8H_4I_2S_6$	$C_{12}F_4N_4{\cdot}2C_8H_4I_2S_6$
M_r	626.36	546.27	1368.70	1368.70
Crystal system, space group	Orthorhombic, *Pbca*	Orthorhombic, *Pnma*	Triclinic, $P\overline{1}$	Triclinic, $P\overline{1}$
Temperature (K)	100	150	293	293
a, b, c (Å)	14.6070 (4), 12.0315 (3), 20.9654 (7)	17.3371 (5), 12.6274 (4), 6.3276 (2)	4.8311 (2), 12.0457 (4), 16.6577 (6)	11.0030 (4), 12.7689 (4), 14.9201 (5)
α, β, γ (°)	90, 90, 90	90, 90, 90	91.128 (2), 92.950 (2), 94.213 (2)	104.906 (2), 106.449 (2), 95.863 (2)
V (Å^3)	3684.55 (18)	1385.25 (7)	965.21 (6)	1907.83 (11)
Z	8	4	1	2
μ (mm^{-1})	4.09	5.41	3.93	3.98
Crystal size (mm)	0.28 × 0.19 × 0.16	0.36 × 0.27 × 0.18	0.24 × 0.08 × 0.05	0.32 × 0.22 × 0.03
Data collection				
Diffractometer	Bruker *APEX*-II CCD	Bruker *APEX*-II CCD	Nonius KappaCCD	Nonius KappaCCD
T_{min}, T_{max}	0.353, 0.520	0.189, 0.377	0.693, 0.822	0.364, 0.888
No. of measured, independent and observed [$I > 2\sigma(I)$] reflections	15 787, 4208, 3600	21 142, 1653, 1581	12 784, 4430, 3215	33 190, 8748, 5762
R_{int}	0.037	0.029	0.040	0.057
$(\sin\theta/\lambda)_{max}$ (Å^{-1})	0.649	0.650	0.650	0.650
Refinement				
$R[F^2 > 2\sigma(F^2)]$, $wR(F^2)$, S	0.030, 0.063, 1.07	0.022, 0.043, 1.12	0.035, 0.082, 1.09	0.057, 0.162, 1.08
No. of reflections	4208	1650	4430	8748
No. of parameters	199	86	235	478
No. of restraints	0	2	0	0
$\Delta\rho_{max}$, $\Delta\rho_{min}$ (e Å^{-3})	1.17, −1.17	0.97, −1.00	0.65, −0.75	1.71, −2.62

Computer programs: *APEX2* (Bruker, 2005), *COLLECT* (Nonius, 1998), *SAINT* (Bruker, 2003), *DIRAX* (Duisenberg, 1992), *SAINT*, *EVALCCD* (Duisenberg *et al.*, 2003), *SIR97* (Altomare *et al.*, 1999), *SHELXL97* (Sheldrick, 2008), *DIAMOND* (Brandenburg & Brendt, 2001), *WinGX* (Farrugia, 2012).

$TCNQF_4$ (2.9 mg, 10.5×10^{-6} mol) in acetonitrile (0.5 ml). Slow diffusion at 293 K afforded black needles after 2 weeks.

2.2.2. Polymorph (II). In a small glass tube of internal diameter 5 mm, a solution of EDT-TTF-I_2 (2.2 mg, 4.0×10^{-6} mol) in 1,1,2-trichloroethane (TCE) was layered with a solution of $TCNQF_4$ (1.7 mg, 6.1×10^{-6} mol) in acetonitrile (0.5 ml). Slow diffusion at 293 K afforded black platelets after 2 weeks.

2.3. Single-crystal X-ray diffraction

For $[NC(CH_2)_2S]_2$-TTF-I_2 and EDT-TTF-I_2, crystals were picked from Paratone® oil with a cryoloop and directly frozen at 150 K under a stream of dry N_2. Data were collected on a Bruker APEX-II CCD diffractometer with κ geometry, using graphite-monochromated Mo $K\alpha$ radiation. For the room-temperature data collections of the two $TCNQF_4$ salts, the crystals were mounted on a thin glass fibre and data were collected on a Nonius KappaCCD diffractometer, also using graphite-monochromated Mo $K\alpha$ radiation. Details of the data collection and refinement parameters are given in Table 1, and displacement ellipsoid plots are shown in Fig. 1. For EDT-TTF-I_2, the molecule lies on a mirror plane, perpendicular to the molecular plane, and the often-encountered disorder of the ethylene group was refined by constraining the site occupancy factors to 0.5 for atoms C5*A* and C5*B* (and their associated H atoms), and restraining the S1–C5*A* and S1–C5*B* bond lengths to be equivalent with an s.u. of 0.01 Å.

2.4. Resistivity measurements

To measure the longitudinal resistivity, gold pads were evaporated on the surface of the crystals in order to improve the quality of the contacts. Then, a standard four-points technique was used with a low frequency lock-in detection (I_{AC} = 0.1–1 µA) for measured resistances below 50 kΩ and DC measurement for higher resistances (I_{DC} = 0.1–0.01 µA). Low temperatures (down to 25 K) were provided by cryo-cooler equipment.

2.5. Theoretical calculations

The tight-binding intermolecular interactions were calculated with the effective one-electron Hamiltonian of the extended Hückel method (Whangbo & Hoffmann, 1978), as implemented in the *Caesar*1.0 chain of programs (Ren *et al.*, 1998). The off-diagonal matrix elements of the Hamiltonian were calculated according to the modified Wolfsberg–Helmholz formula (Ammeter *et al.*, 1978). All valence electrons were explicitly taken into account in the calculations and the basis set consisted of double-ζ Slater-type orbitals for all

Table 2
Averaged bond distances (Å) within the $TCNQF_4$ molecule in selected compounds.

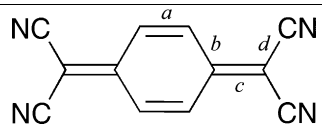

Compound	ρ_{TCNQF4} (assumed)	*a*	*b*	*c*	*d*	ρ_{TCNQF4} (calc)
$TCNQF_4$[a]	0	–	1.372	1.437	1.372	0
Polymorph (I)	−1	1.344	1.420	1.408	1.422	−0.85
Polymorph (II)	−1	1.360	1.4275	1.415	1.4245	−0.88
TBA,$TCNQF_4$[b]	−1	–	1.426	1.418	1.417	−1.0

References: (*a*) Emge *et al.* (1981); (*b*) O'Kane *et al.* (2000).

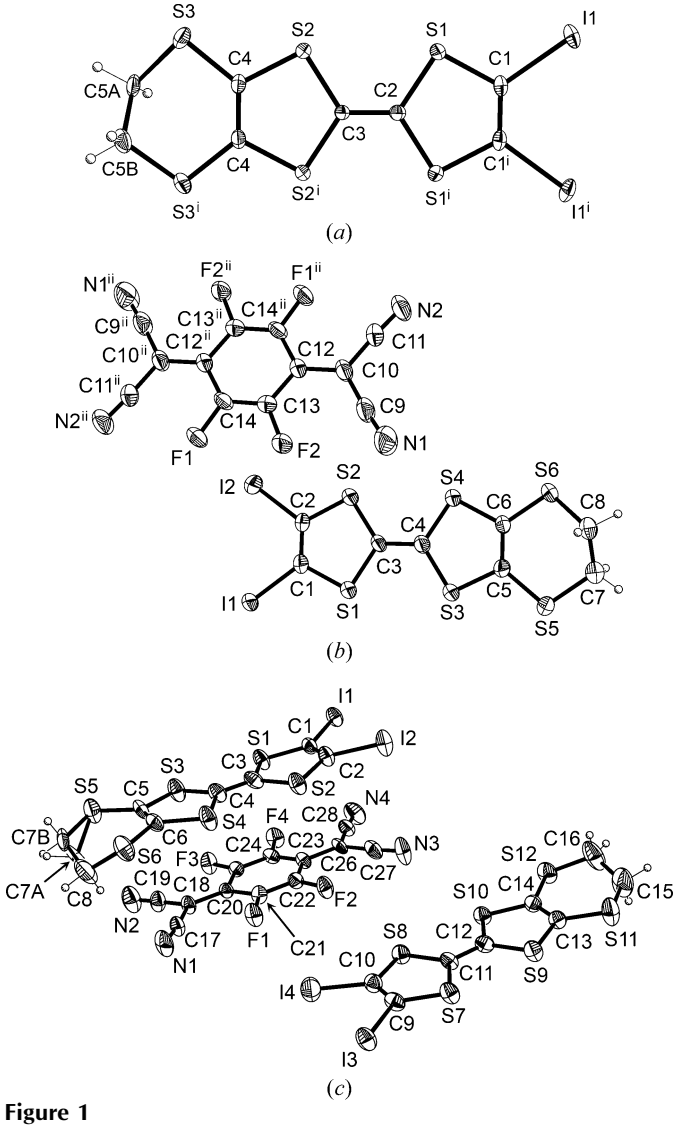

Figure 1
Molecular structures of (*a*) EDT-TTF-I_2, and (*b*) polymorph (I) and (*c*) polymorph (II) of $(EDT\text{-}TTF\text{-}I_2)_2(TCNQF_4)$, showing displacement ellipsoids at 50% probability for non-H atoms. For EDT-TTF-I_2 only one disorder component is shown for the disordered ethylene group (atoms C5*A* and C5*B*). Symmetry codes: (i) $x, \frac{1}{2}-y, z$; (ii) $2-x, 1-y, 1-z$.

atoms except H (ζ Slater-type orbital) using the Roothaan–Hartree–Fock wavefunctions (Clementi & Roetti, 1974).

3. Results and discussion

3.1. The neutral EDT-TTF-I_2 molecule

The structure of the neutral molecule EDT-TTF-I_2 is of interest to determine its geometrical characteristics, particularly the intramolecular bond lengths within the TTF core, as they are known to evolve with the oxidation state of the molecule, with a lengthening of the C═C and concomitant shortening of the C—S bonds upon oxidation. Although many cation radical salts of EDT-TTF-I_2 have been described so far, the structure of the neutral donor molecule was previously unknown. EDT-TTF-I_2 crystallizes in space group *Pnma*, with the crystallographic mirror plane lying perpendicular to the molecular plane (Fig. 1). In the crystal (Fig. 2) the EDT-TTF-I_2 molecules stack into uniform chains along the *c* axis. No short I···I intermolecular contacts are identified. Note that this structure differs from that reported for the analogous dichloro and dibromo derivatives, EDT-TTF-Cl_2 and EDT-TTF-Br_2 (Kux *et al.*, 1995), where head-to-tail dyads were reported to organize into a herringbone structure.

3.2. Polymorph (I): needles of $(EDT\text{-}TTF\text{-}I_2)_2(TCNQF_4)$

Polymorph (I) crystallizes in space group $P\bar{1}$, with the EDT-TTF-I_2 molecule in a general position and the $TCNQF_4$ molecule on an inversion centre, giving the 2:1 stoichiometry (Fig. 1*b*). The charge of $TCNQF_4$ can be estimated by the Kistenmacher relationship first established for TCNQ salts (Kistenmacher *et al.*, 1982) and adapted to $TCNQF_4$ (Miyasaka *et al.*, 2010). It writes as $\rho_{TCNQF4} = A[c/(b+d)] + B$, where *b*–*d* are the intramolecular distances of $TCNQF_4$ defined in Table 2, and *A* and *B* are parameters determined by assuming

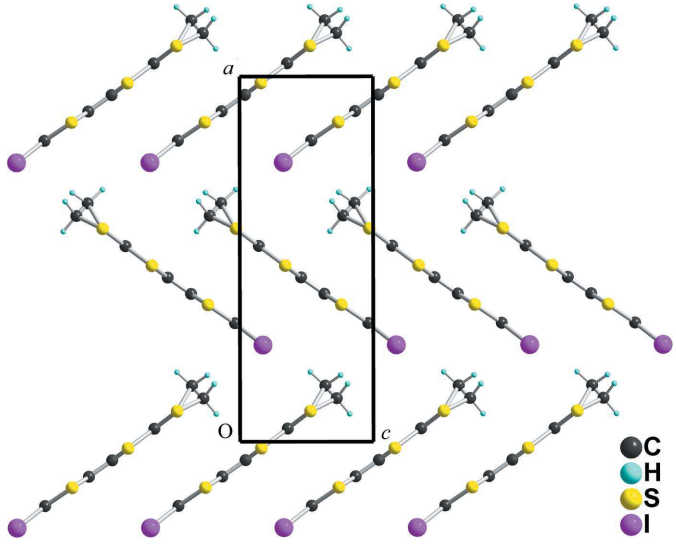

Figure 2
Projection view along *b* of one layer of molecules in the crystal structure of EDT-TTF-I_2.

Table 3
Averaged intramolecular bond distances (Å) within the TTF core in selected compounds, together with estimated (ρ_{est}) and calculated (ρ_{calc}, see text) charges in EDT-TTF-I_2.

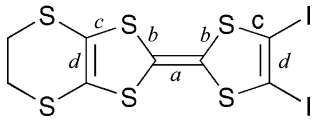

Compound	ρ_{est}	*a*	*b*	*c*	*d*	ρ_{calc}
EDT-TTF-I_2	0	1.351	1.768	1.754	1.3365	+0.07
(EDT-TTF-I_2)$_2I_3$[a]	+0.5	1.365	1.7405	1.749	1.348	+0.55
(EDT-TTF-I_2)$_2$Br·2H_2O[b]	+0.5	1.358	1.7335	1.74625	1.3355	+0.45
(EDT-TTF-I_2)$_2X$[c]†	+0.5	1.36	1.7395	1.74425	1.343	+0.47
Polymorph (I)	+0.5	1.368	1.740	1.747	1.330	+0.51
Polymorph (II)						
mol. *A*	$\simeq 0$	1.344	1.757	1.758	1.354	+0.21
mol. *B*	$\simeq +1$	1.393	1.727	1.735	1.364	+1.12
(EDT-TTF-I_2)ClO_4[d]	+1	1.388	1.727	1.737	1.354	+0.99
(EDT-TTF-I_2)$_2$(2,6-NBS)[d]	+1	1.389	1.73075	1.741	1.359	+0.98
(EDT-TTF-I_2)I_3[a]	+1	1.401	1.7185	1.7335	1.3485	+1.15
(EDT-TTF-I_2)[Ni(mnt)$_2$][e]	+1	1.388	1.731	1.744	1.347	+0.84

References: (*a*) Domercq *et al.* (2001); (*b*) Imakubo *et al.* (2006); (*c*) Hervé *et al.* (2006); (*d*) Shin *et al.* (2011); (*e*) Devic *et al.* (2002). † X = [Cr(NCS)$_4$(isoq)$_2$]$^-$.

a completely neutral (Emge *et al.*, 1981) and a fully ionized (*i.e.* 1 e$^-$ reduced) form of $TCNQF_4$, such as in (^{n}Bu$_4$N)($TCNQF_4$) (O'Kane *et al.*, 2000), giving A = −46.729 and B = 22.308. Applied to polymorph (I), it gives an approximate calculated charge of −0.85, confirming that the $TCNQF_4$ is reduced to the radical anion state, *i.e.* $TCNQF_4^{-\bullet}$. As a consequence, the EDT-TTF-I_2 molecule is only partially oxidized (ρ_{TTF} = +0.5). Comparison of the intramolecular bond distances within the TTF core (Table 3) confirms this assumption, with lengthening of the C=C bonds and shortening of the C−S bonds associated with the partial oxidation, when compared to the neutral donor molecule.

In the solid state the donor and acceptor molecules stack along the *a* axis, giving rise to the formation of (011) layers where a $TCNQF_4$ stack alternates with two neighbouring EDT-TTF-I_2 stacks (Figs. 3 and 4). These layers are interconnected through a particularly short C—I···N≡C halogen-bonding interaction. Indeed, the I···N distance of 2.934 (6) Å is notably shorter than the sum of the van der Waals radii of I (1.98 Å) and N (1.52 Å), hence a reduction parameter, defined as 100× the sum of van der Waals radii over the actual I···N distance, of 84%. Its strength is also demonstrated by its linearity, with a C—I···N angle of 177.3 (2)°, while the I···N≡C angle at 163.9 (5)° shows that the N atom acts as a halogen-bond donor through its lone pair. The I···N distance also compares with those reported (Lieffrig *et al.*, 2013) for the ionic charge-transfer *salts* isolated with $TCNQF_2$ and TCNQF (2.93–2.95 Å), while the neutral charge-transfer *complexes* present longer I···N contacts (> 3.0 Å). This confirms the ionic character of polymorph (I). Note also that this halogen-bonding interaction, combined with the centrosymmetric character of $TCNQF_4$, most probably favours the 2:1 stoichiometry, at variance with the most common charge-transfer salts such as TTF·TCNQ or TTF·chloranil, which have 1:1 stoichiometry.

The mixed-valence character of the EDT-TTF-I_2 stacks suggests that this salt could be conducting. Indeed, it exhibits a room-temperature conductivity (σ_{RT}) of 0.4 S cm^{-1}, while the temperature dependence of the resistivity (Fig. S2 in the supporting information) shows a semiconducting behaviour with a large activation energy, E_a = 0.146 eV (1700 K). Under pressure, σ_{RT} increases up to 0.7 S cm^{-1} at 0.25 GPa (Fig. S3 in the supporting information). Calculations of the $\beta_{HOMO-HOMO}$ interaction energies between neighbouring EDT-TTF-I_2 molecules within these twin stacks show that the strongest interaction is found within the stack, with β_{intra} = −0.18 eV, while the lateral interaction between coplanar EDT-TTF-I_2 molecules, β_{inter}, amounts to +0.091 eV. The system can thus be described as two interacting, non-dimerized, 3/4-filled chains. Such regular chains are currently the subject of strong interest as model systems, since most one-dimensional cation radical salts are slightly dimerized (Hünig & Herverth, 2004;

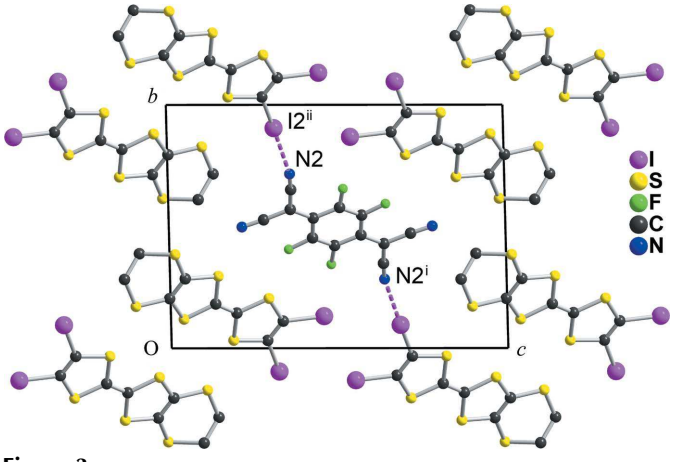

Figure 3
Projection view along *a* of the unit cell of (EDT-TTF-I_2)$_2$($TCNQF_4$), polymorph (I). Symmetry codes: (i) $2-x, 1-y, 1-z$; (ii) $1-x, 1-y, 1-z$.

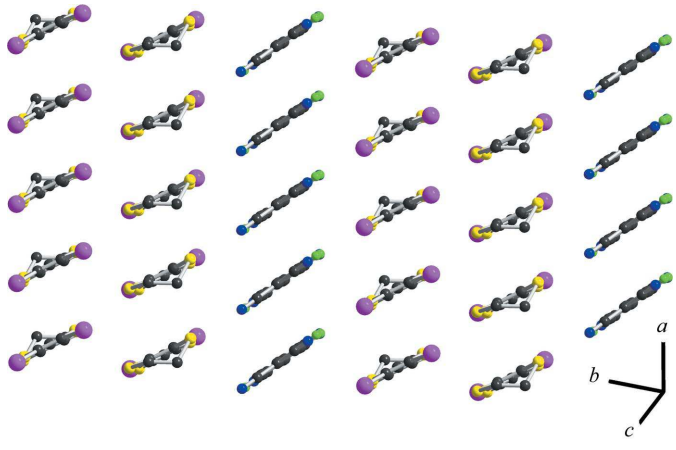

Figure 4
A view along the long molecular axes of both donor and acceptor molecules in (EDT-TTF-I_2)$_2$($TCNQF_4$), polymorph (I), showing alternation of DDA columns in the (011) plane.

Auban-Senzier *et al.*, 2009; Foury-Leylekian *et al.*, 2011). However, the inter-stack coupling between the two inversion-related chains gives rise here to two non-degenerate bands, with the upper one only half-filled (Fig. 5). Under those circumstances, we are brought back to the half-filled systems such as the semiconducting TMTTF series (Pouget, 2012). Note also that $TCNQF_4^{-\bullet}$ most probably does not contribute to the crystal conductivity as the overlap interaction $\beta_{LUMO-LUMO}$ is very weak, +0.005 eV, a consequence of a strongly shifted overlap between molecules (Fig. S4 in the supporting information).

3.3. Polymorph (II): plates of (EDT-TTF-I_2)$_2$($TCNQF_4$)

Polymorph (II) of (EDT-TTF-I_2)$_2$($TCNQF_4$) also crystallizes in space group $P\bar{1}$, but with two crystallographically independent donor molecules, together with a $TCNQF_4$ molecule in a general position (Figs. 1*c* and 6). The $TCNQF_4$ molecules are organized into centrosymmetric dimers, stacking with centrosymmetric EDT-TTF-I_2 tetramers along the [201] direction (Fig. 7). Those layers are connected to each other by the halogen-bonding interactions shown in Fig. 5. This motif is quite similar to that observed in polymorph (I), but its supramolecular organization differs completely (see below). Note, however, that the I···N distances, notably shorter than 3 Å, are in accordance with the ionic nature of this compound.

As already detailed for polymorph (I), the analysis of the intramolecular bond distances within both donor and acceptor molecules helps to assess their charge. For $TCNQF_4$, application of the formula used in Table 2 shows that the acceptor molecule is again fully reduced to the radical anion state, $TCNQF_4^{-\bullet}$. At variance with polymorph (I), however, this does not imply a +0.5 charge for the two EDT-TTF-I_2 molecules, there are now two crystallographically independent donor molecules. Inspection of the central C═C bond length (Table 3), shows that molecule *B* [C11═C12 1.393 (12) Å] is probably more oxidized than molecule *A*, which exhibits a shorter C3═C4 bond [1.344 (12) Å]. In order to assess in a more precise way the actual charge of both donor molecules, we have developed a correlation between intramolecular bond length and charge, by analogy with those reported for BEDT-TTF (Guionneau *et al.*, 1997). This becomes possible with the structural characterization of the neutral molecule reported above, complemented by structural data for selected EDT-TTF-I_2 salts (Table 3) where the oxidation state of the molecule is unambiguous, that is within those structures with only one crystallographically independent molecule. Our correlation between bond distances and charges, based on neutral

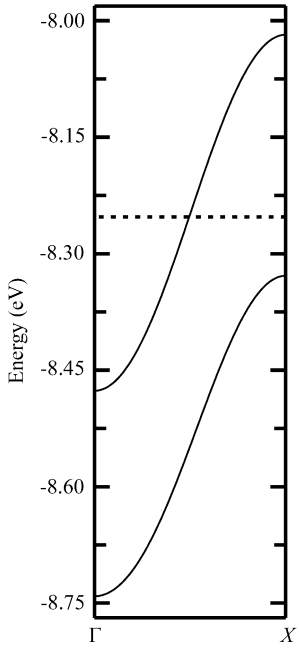

Figure 5
Calculated band structure for the one-dimensional EDT-TTF-I_2 system in polymorph (I). The dotted line indicates the Fermi level for the hypothetical metallic state.

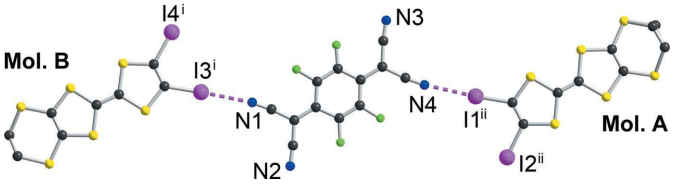

Figure 6
Halogen-bonded motifs in (EDT-TTF-I_2)$_2$($TCNQF_4$) polymorph (II). Halogen bonds are shown as purple dotted lines and H atoms are omitted. Symmetry codes: (i) $1-x, -y, 1-z$; (ii) $2-x, 2-y, 1-z$.

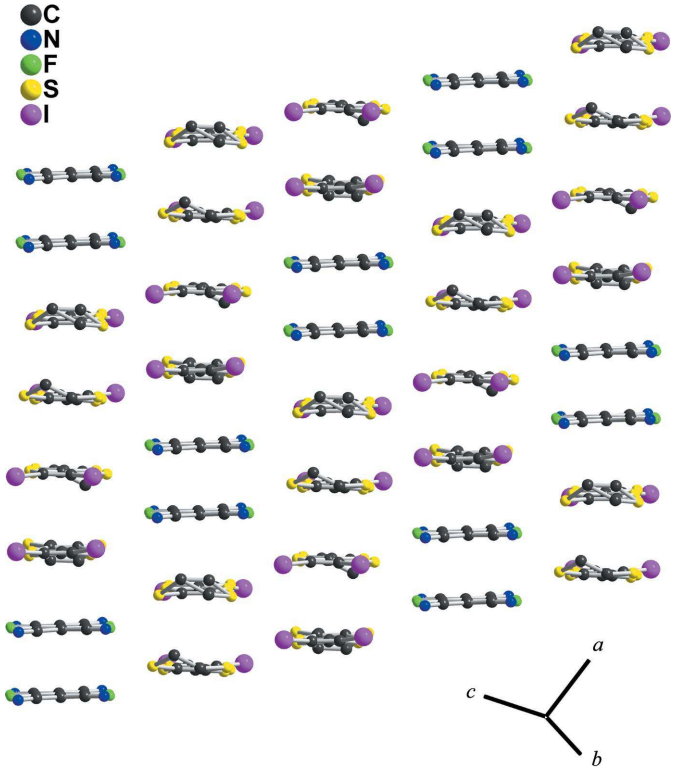

Figure 7
View along the long molecular axes of both donor and acceptor molecules in (EDT-TTF-I_2)$_2$($TCNQF_4$) polymorph (II), showing the alternating $\ldots D_4A_2D_4A_2\ldots$ columns of molecules stacking along [201].

EDT-TTF-I_2, partially oxidized (ρ = +0.5) and fully oxidized (ρ = +1) EDT-TTF-I_2 salts, is $\rho_{cal} = A + B[(b + c) - (a + d)]$, with A = 6.8617 and B = −8.1332. Applied to the two crystallographically independent EDT-TTF-I_2 molecules in polymorph (II), it gives $\rho_{calc}(A)$ = +0.21 and $\rho_{calc}(B)$ = +1.12, confirming that molecule A is essentially neutral while molecule B is fully oxidized to the radical cation state.

This strong charge ordering has a striking influence on the solid-state association of the EDT-TTF-I_2 molecules in the salt. As shown in Fig. 8, the two singly oxidized B molecules form an almost perfectly eclipsed face-to-face dyad (Fig. 8*b*). This leads to strong overlap between the π-type SOMO, with the bonding combination occupied by two electrons, a prototype of a single $2e^-$ σ bond (Fourmigué, 2012), delocalized between the two molecules. These diamagnetic dyads are surrounded by two essentially neutral EDT-TTF-I_2 molecules, alternating then along the stacking direction with $TCNQF_4$ dyads (Fig. 7). In the latter, the face-to-face association of $TCNQF_4$ radical anions detailed in Fig. 9 corresponds most probably (see below) to a strong interaction between LUMOs.

Calculations of the interaction energies, $\beta_{HOMO-HOMO}$ and $\beta_{LUMO-LUMO}$, confirm these assumptions. For the donor's HOMO, the β_{BB} interaction energy amounts to −0.95 eV while by contrast β_{AB} is only −0.35 eV. A large $\beta_{LUMO-LUMO}$ for the bond-over-ring overlap is also calculated for the $TCNQF_4$ dimers, with $\beta_{LUMO-LUMO}$ = +0.46 eV. This strong pairing of both radical species into bonding combinations of the singly occupied molecular orbitals lets us infer a diamagnetic, insulating character for polymorph (II).

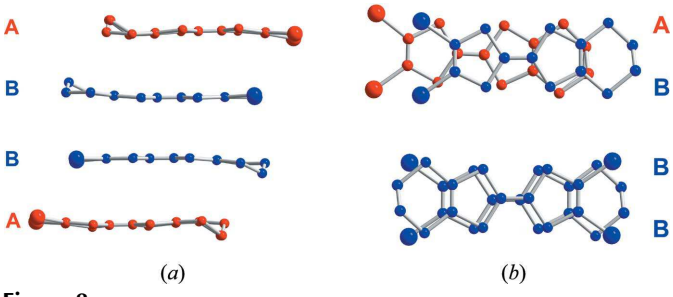

Figure 8
(*a*) Side view of the EDT-TTF-I_2 tetramers, showing the distortions from planarity of the essentially neutral donors A (in red), interacting with oxidized B molecules (in blue). (*b*) Projection view of the AB and BB overlaps within the tetramer, showing the eclipsed BB overlap characteristic of dicationic dimers.

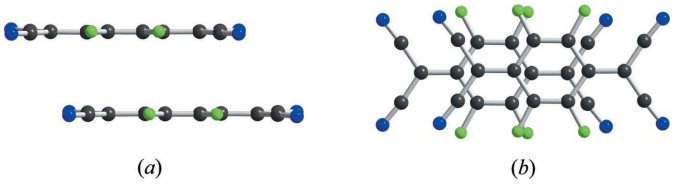

Figure 9
(*a*) Side view of the $TCNQF_4$ dimer in polymorph (II). (*b*) Projection view of the $TCNQF_4$ dimer in polymorph (II), showing the bond-over-ring overlap pattern.

3.4. The halogen-bond interaction

Comparison of the two polymorphs shows that the I···N distances in both cases are essentially the same, whatever the charge of the EDT-TTF-I_2 molecule: 2.934 (6) Å for a charge +0.5 in polymorph (I), and 2.933 (9) and 2.949 (9) Å, respectively, for the EDT-TTF-I_2 molecules with charges 0 and +1 in polymorph (II). It has recently been shown, however, that in isostructural systems with variable charge, there is indeed a direct correlation between charge and halogen-bond lengths (Lieffrig *et al.*, 2013). The similar halogen-bond distances observed here might therefore be only a consequence of the different crystal packing. It also indicates that it is essentially the negative charge of the $TCNQF_4^{-\bullet}$ radical anion which contributes strongly to the halogen-bond strength, while the I atoms are only weakly activated upon TTF oxidation. This feature was already noted in the charge-transfer salts of the monoiodo TTF derivative, EDT-TTF-I (Lieffrig, Jeannin, Guizouarn *et al.*, 2012; Lieffrig, Jeannin, Shin *et al.*, 2012), The strengthening of the halogen bond in such systems when turning from neutral to ionic is therefore essentially attributable to the negative charge which develops on the halogen-bond acceptor, here the nitrile substituent of $TCNQF_4$.

4. Conclusion

We have shown that halogen bonding with iodinated tetrathiafulvalenes is a very efficient structural tool to associate these donor molecules, not only with counter ions in cation radical salts but also with electroactive anions in charge-transfer salts. The symmetry of the TCNQ derivatives, here $TCNQF_4$, favours the formation of 2:1 salts, at variance with the prototypical TTF·TCNQ or TTF·chloranil where both partners have the same symmetry. With strong acceptors such as $TCNQF_4$, it leads to a mixed-valence state for the donor molecules, a radical state which is stabilized through two very different ways. In polymorph (I) of $(EDT\text{-}TTF\text{-}I_2)_2(TCNQF_4)$, the formation of segregated stacks of donor and acceptor molecules allows the radicals to delocalize into partially filled bands. On the other hand, in polymorph (II), we observe a complete charge separation, with one neutral (D^0) and one fully oxidized ($D^{+\bullet}$) donor molecule, together with the formation of localized two-electron bonds, in D_2^{2+} and A_2^{2-} species. This very different solid-state organization of the halogen-bonded D–A–D trimetric motifs provides a textbook example of two modes of face-to-face interaction between π-type radicals, either delocalized, uniform chains with partial charge transfer and conducting behaviour, or localized association of radicals into face-to-face dyads. It also demonstrates that charge-assisted halogen bonding relies essentially on the negative charge of the halogen-bond acceptor (the Lewis base), rather than on the partial positive charge of the I atoms, at least in these TTF-based systems. Comparison with halogenated cations such as iodopyridinium (Derossi *et al.*, 2009) or diiodopyridinium (Derossi *et al.*, 2009; Kosaka *et al.*, 2007, 2013) salts could provide interesting answers to this point.

Financial support from the ANR (Paris, France) under contract No. ANR-08-BLAN-0091–02 is acknowledged. We also thank the X-ray facility in Rennes (Th. Roisnel, CDIFX) for providing access to diffractometers.

References

Alberola, A., Collis, R. J., García, F. & Howard, R. E. (2006). *Tetrahedron*, **62**, 8152–8157.

Alberola, A., Fourmigué, M., Gómez-García, C. J., Llusar, R. & Triguero, S. (2008). *New J. Chem.* **32**, 1103–1109.

Altomare, A., Burla, M. C., Camalli, M., Cascarano, G. L., Giacovazzo, C., Guagliardi, A., Moliterni, A. G. G., Polidori, G. & Spagna, R. (1999). *J. Appl. Cryst.* **32**, 115–119.

Ammeter, J. H., Buergi, H. B., Thibeault, J. C. & Hoffmann, R. (1978). *J. Am. Chem. Soc.* **100**, 3686–3692.

Auban-Senzier, P., Pasquier, C. R., Jérome, D., Suh, S., Brown, S. E., Mézière, C. & Batail, P. (2009). *Phys. Rev. Lett.* **102**, 257001.

Batsanov, A. S., Bryce, M. R., Chesney, A., Howard, J. A. K., John, D. E., Moore, A. J., Wood, C. L., Gershtenman, H., Becker, J. Y., Khodorkovsky, V. Y., Ellern, A., Bernstein, J., Perepichka, I. F., Rotello, V., Gray, M. & Cuello, A. O. (2001). *J. Mater. Chem.* **11**, 2181–2191.

Brandenburg, K. & Brendt, M. (2001). *DIAMOND*, Release 2, 1e. Crystal Impact GbR, Bonn, Germany.

Bruckmann, A., Pena, M. A. & Bolm, C. (2008). *Synlett*, **6**, 900–902.

Bruker (2003). *SADABS* and *SAINT*. Bruker AXS Inc., Madison, Wisconsin, USA.

Bruker (2005). *APEX2*. Bruker AXS Inc., Madison, Wisconsin, USA.

Cariati, E., Forni, A., Biella, S., Metrangolo, P., Meyer, F., Resnati, G., Righetto, S., Tordin, E. & Ugo, R. (2007). *Chem. Commun.* **25**, 2590–2592.

Cavallo, G., Metrangolo, P., Pilati, T., Resnati, G., Sansotera, M. & Terraneo, G. (2010). *Chem. Soc. Rev.* **39**, 3772–3783.

Clementi, E. & Roetti, C. (1974). *At. Data Nucl. Data Tables*, **14**, 177–478.

Derossi, S., Brammer, L., Hunter, C. A. & Ward, M. D. (2009). *Inorg. Chem.* **48**, 1666–1677.

Devic, T., Domercq, B., Auban-Senzier, P., Molinié, P. & Fourmigué, M. (2002). *Eur. J. Inorg. Chem.* pp. 2844–2849.

Devic, T., Evain, M., Moëlo, Y., Canadell, E., Auban-Senzier, P., Fourmigué, M. & Batail, P. (2003). *J. Am. Chem. Soc.* **125**, 3295–3301.

Domercq, B., Devic, T., Fourmigué, M., Auban-Senzier, P. & Canadell, E. (2001). *J. Mater. Chem.* **11**, 1570–1575.

Duisenberg, A. J. M. (1992). *J. Appl. Cryst.* **25**, 92–96.

Duisenberg, A. J. M., Kroon-Batenburg, L. M. J. & Schreurs, A. M. M. (2003). *J. Appl. Cryst.* **36**, 220–229.

Emge, T., Maxfield, M., Cowan, D. & Kistenmacher, T. (1981). *Mol. Cryst. Liq. Cryst.* **65**, 161–178.

Farrugia, L. J. (2012). *J. Appl. Cryst.* **45**, 849–854.

Fourmigué, M. (2008). *Struct. Bond.* **126**, 181–207.

Fourmigué, M. (2012). *The Importance of π-Interactions in Crystal Engineering: Frontiers in Crystal Engineering*, edited by E. Tiekink & J. Zukerman-Schpector, 2nd ed, Ch. 6, pp. 143–162. New York: John Wiley and Sons Ltd.

Fourmigué, M. & Auban-Senzier, P. (2008). *Inorg. Chem.* **47**, 9979–9986.

Fourmigué, M. & Batail, P. (2004). *Chem. Rev.* **104**, 5379–5418.

Foury-Leylekian, P., Auban-Senzier, P., Coulon, C., Jeannin, O., Fourmigué, M., Pasquier, C. & Pouget, J.-P. (2011). *Phys. Rev. B*, **84**, 195134.

Gilday, L. C., Lang, T., Caballero, A., Costa, P. J., Félix, V. & Beer, P. D. (2013). *Angew. Chem. Int. Ed.* **52**, 4356–4360.

Gompper, R., Hock, J., Polborn, K., Dormann, E. & Winter, H. (1995). *Adv. Mater.* **7**, 41–43.

Guionneau, P., Kepert, C. J., Bravic, G., Chasseau, D., Truter, M. R., Kurmoo, M. & Day, P. (1997). *Synth. Met.* **86**, 1973–1974.

Hervé, K., Cador, O., Golhen, S., Costuas, K., Halet, J.-F., Shirahata, T., Muto, T., Imakubo, T., Miyazaki, A. & Ouahab, L. (2006). *Chem. Mater.* **18**, 790–797.

Hünig, S. & Herverth, E. (2004). *Chem. Rev.* **104**, 5535–5564.

Imakubo, T., Sawa, H. & Kato, R. (1995). *Synth. Met.* **73**, 117–122.

Imakubo, T., Shirahata, T., Hervé, K. & Ouahab, L. (2006). *J. Mater. Chem.* **16**, 162–173.

Kistenmacher, T. J., Emge, T. J., Bloch, A. N. & Cowan, D. O. (1982). *Acta Cryst.* B**38**, 1193–1199.

Kniep, F., Jungbauer, S. H., Zhang, Q., Walter, S. M., Schindler, S., Schnapperelle, I., Herdtweck, E. & Huber, S. M. (2013). *Angew. Chem. Int. Ed.* **52**, 7028–7032.

Kosaka, Y., Yamamoto, H. M., Nakao, A., Tamura, M. & Kato, R. (2007). *J. Am. Chem. Soc.* **129**, 3054–3055.

Kosaka, Y., Yamamoto, H. M., Tajima, A., Nakao, A., Cui, H. & Kato, R. (2013). *CrystEngComm*, **15**, 3200–3211.

Kux, U., Suzuki, H., Sasaki, S. & Iyoda, M. (1995). *Chem. Lett.* pp. 183–184.

Lieffrig, J., Jeannin, O., Frąckowiak, A., Olejniczak, I., Świetlik, R., Dahaoui, S., Aubert, E., Espinosa, E., Auban-Senzier, P. & Fourmigué, M. (2013). *Chem. Eur. J.* **19**, 14804–14813.

Lieffrig, J., Jeannin, O., Guizouarn, T., Auban-Senzier, P. & Fourmigué, M. (2012). *Cryst. Growth Des.* **12**, 4248–4257.

Lieffrig, J., Jeannin, O., Shin, K.-S., Auban-Senzier, P. & Fourmigué, M. (2012). *Crystals*, **2**, 327–337.

Meazza, L., Foster, J. A., Fucke, K., Metrangolo, P., Resnati, G. & Steed, J. W. (2013). *Nat. Chem.* **5**, 42–47.

Metrangolo, P., Meyer, F., Pilati, T., Resnati, G. & Terraneo, G. (2008). *Angew. Chem. Int. Ed.* **47**, 6114–6127.

Metrangolo, P., Pilati, T., Terraneo, G., Biella, S. & Resnati, G. (2009). *CrystEngComm*, **11**, 1187–1196.

Metrangolo, P., Präsang, C., Resnati, G., Liantonio, R., Whitwood, A. C. & Bruce, D. W. (2006). *Chem. Commun.* **31**, 3290–3292.

Metrangolo, P. & Resnati, G. (2001). *Chem. Eur. J.* **7**, 2511–2519.

Metrangolo, P. & Resnati, G. (2012). *Cryst. Growth Des.* **12**, 5835–5838.

Meyer, F. & Dubois, P. (2013). *CrystEngComm*, **15**, 3058–3071.

Miyasaka, H., Motokawa, N., Matsunaga, S., Yamashita, M., Sugimoto, K., Mori, T., Toyota, N. & Dunbar, K. R. (2010). *J. Am. Chem. Soc.* **132**, 1532–1544.

Nguyen, H. L., Horton, P. N., Hursthouse, M. B., Legon, A. C. & Bruce, D. W. (2004). *J. Am. Chem. Soc.* **126**, 16–17.

Nonius (1998). *COLLECT*. Nonius BV, Delft, The Netherlands.

O'Kane, S. A., Clérac, R., Zhao, H., Ouyang, X., Galán-Mascarós, J. R., Heintz, R. & Dunbar, K. R. (2000). *J. Solid State Chem.* **152**, 159–173.

Pouget, J.-P. (2012). *Crystals*, **2**, 466–520.

Präsang, C., Whitwood, A. C. & Bruce, D. W. (2008). *Chem. Commun.* **18**, 2137–2139.

Ranganathan, A., El-Ghayoury, A., Meziere, C., Harté, E., Clérac, R. & Batail, P. (2006). *Chem. Commun.* pp. 2878–2880.

Ren, J., Liang, W. & Whangbo, M.-H. (1998). *CAESAR*. PrimeColor Software, Inc. Cary, North Carolina, USA.

Sheldrick, G. M. (2008). *Acta Cryst.* A**64**, 112–122.

Shin, K.-S., Brezgunova, M., Jeannin, O., Roisnel, T., Camerel, F., Auban-Senzier, P. & Fourmigué, M. (2011). *Cryst. Growth Des.* **11**, 5337–5345.

Ueda, K., Sugimoto, T., Faulmann, C. & Cassoux, P. (2003). *Eur. J. Inorg. Chem.* pp. 2333–2338.

Walter, S. M., Kniep, F., Herdtweck, E. & Huber, S. M. (2011). *Angew. Chem. Int. Ed.* **50**, 7187–7191.

Wang, C., Ellern, A., Khodorkovsky, V., Bernstein, J. & Becker, J. Y. (1994). *J. Chem. Soc. Chem. Commun.* pp. 983–984.

Whangbo, M. & Hoffmann, R. (1978). *J. Am. Chem. Soc.* **100**, 6093–6098.

Wheland, R. C. & Martin, E. L. (1975). *J. Org. Chem.* **40**, 3101–3109.